

Energetic particle precipitation in ECHAM5/MESSy1 – Part 1: Downward transport of upper atmospheric NO_x produced by low energy electrons

A. J. G. Baumgaertner, P. Jöckel, and C. Brühl

Max Planck Institute for Chemistry, Mainz, Germany

Received: 2 October 2008 – Published in Atmos. Chem. Phys. Discuss.: 18 December 2008

Revised: 25 March 2009 – Accepted: 18 April 2009 – Published: 24 April 2009

Abstract. The atmospheric chemistry general circulation model ECHAM5/MESSy1 has been extended by processes that parameterise particle precipitation. Several types of particle precipitation that directly affect NO_y and HO_x concentrations in the middle atmosphere are accounted for and discussed in a series of papers. In the companion paper, the ECHAM5/MESSy1 solar proton event parametrisation is discussed, while in the current paper we focus on low energy electrons (LEE) that produce NO_x in the upper atmosphere. For the flux of LEE NO_x into the top of the model domain a novel technique which can be applied to most atmospheric chemistry general circulation models has been developed and is presented here. The technique is particularly useful for models with an upper boundary between the stratopause and mesopause and therefore cannot directly incorporate upper atmospheric NO_x production. The additional NO_x source parametrisation is based on a measure of geomagnetic activity, the A_p index, which has been shown to be a good proxy for LEE NO_x interannual variations. HALOE measurements of LEE NO_x that has been transported into the stratosphere are used to develop a scaling function which yields a flux of NO_x that is applied to the model top. We describe the implementation of the parametrisation as the sub-model SPACENOX in ECHAM5/MESSy1 and discuss the results from test simulations. The NO_x enhancements are shown to be in good agreement with independent measurements. A_p index data is available for almost one century, thus the parametrisation is suitable for simulations of the recent climate.

1 Introduction

Since the 1980's measurements and models have shown that under certain circumstances, NO_x produced in the thermosphere by precipitating low energy electrons (LEE) can be transported downward into the stratosphere and there engage in catalytic ozone destruction (Brasseur and Solomon, 1986; Callis et al., 1998; Callis and Lambeth, 1998; Callis et al., 2001, 2002; Randall et al., 2007; Funke et al., 2005). There is emerging evidence that this is an important process amongst several sun-earth connection mechanisms (e.g. Rozanov et al., 2005). The electrons originate at the sun and from magnetospheric reservoirs, and precipitate at high latitudes during times of enhanced geomagnetic activity. In terms of stratospheric NO_x production, Funke et al. (2005) found electrons with energies up to approximately 30 keV, which deposit their energy above 90 km, to be the most relevant. There they lead to the production of NO_x through dissociation and ionization processes (Rusch et al., 1981). In the polar winter, where the photochemical loss of NO_x is negligible and where the Brewer-Dobson circulation leads to a downward transport, NO_x enhancements can be transported down into the stratosphere and lead to significant ozone loss. This has been termed the energetic particle precipitation (EPP) indirect effect by Randall et al. (2007), in contrast to the EPP direct effect where NO_x and HO_x are produced in the middle atmosphere mainly through highly energetic electrons and protons.

Measurements of enhancements of NO_x formed by low energy electrons (LEE NO_x) have been made by a growing number of instruments. The Limb Infrared Monitor of the Stratosphere (LIMS) observed NO₂ mixing ratios of up to 175 ppbv in the 1978/1979 winter (Russell et al., 1988). The fact that such enhancements of NO_x occur on a regular basis was realized when the Halogen Occultation Experiment (HALOE) data became available. Such observations



Correspondence to:
A. J. G. Baumgaertner
(abaumg@mpch-mainz.mpg.de)

are for example described in Siskind et al. (2000), Hood and Soukharev (2006) and Randall et al. (2007). Other studies of this type include Randall et al. (1998), who showed NO₂ enhancements using the Polar Ozone and Aerosol Measurement (POAM II) instrument and Rinsland et al. (1999), who reported polar winter NO_y descent seen by the Atmospheric Trace Molecule Spectroscopy (ATMOS) instrument on board the space shuttle.

An extensive study using the Michelson Interferometer for Passive Atmospheric Sounding (MIPAS) on board ENVISAT by Funke et al. (2005) clearly showed NO_x enhancements in the 2003 Southern Hemisphere winter stratosphere with mixing ratios of up to 200 ppbv. Seppälä et al. (2007) used GOMOS and POAM III measurements to show that the descent of LEE NO_x can be a major contributor to stratospheric NO_x enhancements also in the Northern Hemisphere.

Only recently studies have been able to argue conclusively that stratospheric NO_x enhancements due to LEE are linked to geomagnetic activity. Such results are for example presented in Siskind et al. (2000), Hood and Soukharev (2006), and Randall et al. (2007). As a measure for global geomagnetic activity often the A_p index is employed. The A_p index is derived from magnetic field component measurements at 13 subauroral geomagnetic observatories (Mayaud, 1980).

In addition to geomagnetic activity, meteorological conditions can have a significant effect on the amount of NO_x found in the polar stratosphere. A stronger and better isolated polar vortex enhances the descent of NO_x from the mesosphere and thermosphere. Especially in the Arctic, where dynamical variability is greater than in the Southern Hemisphere, this can occasionally lead to pronounced NO_x enhancements that are not linked to geomagnetic activity, as has been shown by Randall et al. (2006).

Treatment of an additional NO_x source in the mesosphere and thermosphere in models has been neglected apart from very few sensitivity studies. Siskind et al. (1997) used a two-dimensional chemical transport model which included E-region chemistry and an ionization source due to auroral particles. However, problems with the model dynamics prevented a good agreement with HALOE data. A very recent study by Vogel et al. (2008) shows Arctic Winter 2003/04 ozone loss resulting from mesospheric NO_x. The CLaMS model in combination with MIPAS satellite data were employed and a significant impact on stratospheric ozone as well as on total column ozone were found. An idealised NO_x source in the upper mesosphere representing relativistic electron precipitation (REP) was implemented into the Freie Universität Berlin Climate Middle Atmosphere Model with online chemistry (FUB-CMAM-CHEM) by Langematz et al. (2005). Although the source was likely to be overestimated, the results showed that the mechanism is important for ozone chemistry. A positive response was reported for ozone at high latitudes at 40–45 km, and a negative response for the tropical lower stratosphere.

Here, we describe a simple parametrisation for NO_x produced by LEE for use in atmospheric chemistry general circulation models (AC-GCMs). The combination of the Modular Earth Submodel System (MESSy) and the general circulation model ECHAM5 is briefly introduced in Sect. 2.1. Due to the fact that the upper boundary of ECHAM/MESSy (EMAC) in the MA (middle atmosphere) setup is located at 0.01 hPa, the AC-GCM is well suited for this study. The parametrisation and its implementation in EMAC in form of the submodel SPACENOX are described in Sect. 2.2. The evaluation and the discussion of the results are presented in Sect. 3.

2 Model description

2.1 ECHAM5/MESSy1

The ECHAM/MESSy Atmospheric Chemistry (EMAC) model is a numerical chemistry and climate simulation system that includes submodels describing tropospheric and middle atmosphere processes and their interaction with oceans, land and human influences (Jöckel et al., 2006). It uses the first version of the Modular Earth Submodel System (MESSy1) to link multi-institutional computer codes. The core atmospheric model is the 5th generation European Centre Hamburg general circulation model (ECHAM5, Roeckner et al. (2006)). The model has been shown to consistently simulate key atmospheric tracers such as ozone (Jöckel et al., 2006), water vapour (Lelieveld et al., 2007), and lower and middle stratospheric NO_y (Brühl et al., 2007). For the present study we applied EMAC (ECHAM5 version 5.3.01, MESSy version 1.6) in the T42L90MA-resolution, i.e. with a spherical truncation of T42 (corresponding to a quadratic gaussian grid of approximately 2.8 by 2.8 degrees in latitude and longitude) with 90 vertical hybrid pressure levels up to 0.01 hPa. This part of the setup matches the model evaluation study by Jöckel et al. (2006). Enabled submodels are also the same as in Jöckel et al. (2006) apart from the new submodels SPE and SPACENOX, a more detailed treatment of the solar variation in the photolysis submodel JVAL, and the sub-submodel FUBRad (Nissen et al., 2007), a high-resolution short-wave heating rate parametrisation. The submodel SPE is described in the companion paper (Baumgaertner et al., 2009), SPACENOX is described here. The chosen chemistry scheme for the configuration of the submodel MECCA1 (Sander et al., 2005) is simpler compared to the configuration in Jöckel et al. (2006). For example, the non-methane hydrocarbon chemistry is not treated at the same level of detail. The complete mechanism is documented in the supplement to this paper at <http://www.atmos-chem-phys.net/9/2729/2009/acp-9-2729-2009-supplement.zip>.

2.2 The submodel SPACENOX

The focus of this work is to study the interannual variability of LEE NO_x and its temporal and spatial behavior during the polar winter. Randall et al. (1998), Randall et al. (2007) and Siskind et al. (2000) have shown that the A_p index is in general sufficient to describe measured interannual variations in the southern polar vortex. Neither seasonal nor interannual variations of the transport between the source region and the model top, i.e. the lower thermosphere (LT), can be captured if the A_p index is used as the only input variable. Seasonal variations of this transport are in the model parametrised using a sinusoidal time dependency (see below). Interannual variations of transport in the LT are not considered, based on the fact that a good agreement between interannual variations of A_p and stratospheric NO_x enhancements was found by the authors mentioned above, and because of the lack of a long term dataset for vertical transport in the lower thermosphere. In the mesosphere, which is mostly captured by the model, and the stratosphere, variations in the strength of the Southern Hemisphere polar vortex are known to be small, but any interannual variations present in the model do not correlate with observed vortex strength because the model simulations presented here are not relaxed to observations. Other forcings, such as sea surface temperatures and chemistry boundary conditions, are not sufficient to reproduce observed vortex variability, such as the sudden warming in 2002.

For the Northern Hemisphere, where dynamic variability is much more pronounced than in the Southern Hemisphere, less evidence exists for a simple relationship between the A_p index and stratospheric NO_x enhancements. Therefore, emphasis here will be on the Southern Hemisphere, while aspects with respect to the implementation of the parametrisation for the Northern Hemisphere as well as results from that area will only be discussed briefly.

Because of the observed direct relationship between the A_p index and NO_x enhancements, the A_p index was chosen as the only required time-varying input for the parametrisation.

In order to obtain the measured NO_x mixing ratios in the model stratosphere, the A_p index needs to be scaled appropriately to yield the required NO flux at the model top. Estimates of NO_x produced in the thermosphere and transported downward into the southern polar stratosphere have been derived from HALOE measurements by Randall et al. (2007), hereafter referred to as R07. Their results cover the years 1992 to 2005 and thus cover more than one solar cycle. This is probably the longest time series of such measurements available. It encompasses the entire spectrum of geomagnetic activity and the A_p index, which has been shown to have a superimposed variation of the time scale of the length of the solar cycle.

In order to develop a scaling function for the flux at the model top, the A_p index was averaged over the period from May to July to yield annual mean values. This time series

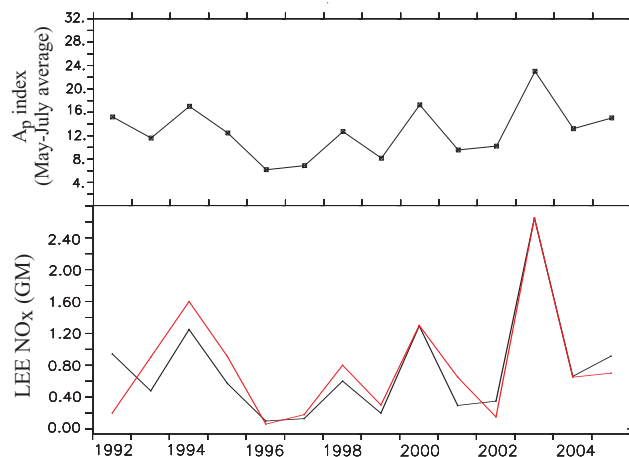


Fig. 1. Top: May–July average A_p index, bottom: LEE NO_x derived from the A_p index (black line) and maximum annual LEE NO_x after R07 (red line).

was fitted to the amount of average annual excess NO_x below 45 km presented in R07 (their Fig. 9), derived there from deviations from the standard low NO_x versus low CH₄ relation. Using a least squares fitting algorithm this yields the function

$$f_{\text{LEE-NOX}}(A_p) = A_p^{2.5} \cdot 1.04 \times 10^{-3} \cdot 1\text{GM}. \quad (1)$$

Note that since A_p is dimensionless the scaled result is multiplied by 1 GM to yield LEE NO_x with unit giga moles (GM). Figure 1 (top) depicts the May–July average A_p index, Fig. 1 (bottom) shows LEE NO_x derived using Eq. (1) (black) and average annual LEE NO_x after R07 (red). The good agreement indicates that in the Southern Hemisphere the interannual variability of the downward transport in the polar vortex is small, so that almost all of the variability can be explained by the variations in geomagnetic activity.

In order to derive a flux of NO_x, excess NO_x densities need to be considered. Similar to above, the scaling function is derived using the data from R07. Because the time resolution of the flux is desired to be higher than yearly, the A_p index was averaged over 2-week periods in order to be compatible with the results from R07 Fig. 7, reproduced here as Fig. 6. Then, $A_p^{2.5} \cdot a \cdot \text{cm}^{-3}$ was fitted to yearly maximum values of R07 Fig. 7 yielding $a = 2.20 \cdot 10^5$. Then excess NO_x densities $g_{\text{LEE-NOX}}$ are

$$g_{\text{LEE-NOX}}(A_p) = A_p^{2.5} \cdot 2.20 \times 10^5 \text{cm}^{-3}. \quad (2)$$

For the flux calculation the following information is needed: (1) excess densities $g_{\text{LEE-NOX}}$, (2) an average vertical velocity, (3) a loss factor which accounts for transport out of the polar night region. Instead of making assumptions about the latter two, which would be error-prone, a trial-and-error approach was chosen in order to get results at 45 km

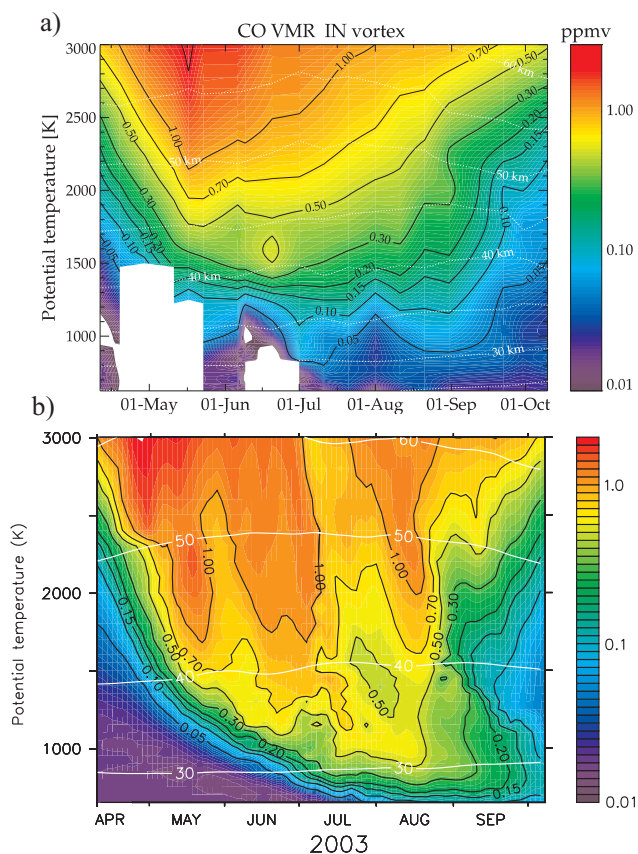


Fig. 2. MIPAS IMK/IAA (a) and EMAC (b) CO mixing ratios (ppmv) inside the southern polar vortex during the Southern Hemisphere winter 2003. The vortex edge was defined using the Nash criterion. The white contour lines denote the altitude in km. (a) reproduced from Funke et al. (2005) with kind permission from AGU and B. Funke.

that match the observations. Therefore, a value for the combination of the latter factors was established through a series of test simulations. Several EMAC simulations with a variable factor c (see Eq. 3) were conducted for the year 2003 in lower vertical resolution with 39 levels (T42L39, model top also at 0.01 hPa). Model excess NO_x densities at 45 km were calculated by subtracting densities from a reference simulation with the submodel turned off. Then, model excess NO_x were compared to the results of R07 (their Fig. 7). The required flux was then determined to be

$$F = A_p^{2.5} \cdot c \cdot 2.20 \times 10^5 \text{ cm}^{-2} \text{ s}^{-1} \quad (3)$$

where $c=0.23$ for “average excess NO_x” (see Fig. 6, or Fig. 7 of R07) and $c=0.45$ for “maximum excess NO_x”.

The transport to lower altitudes only acts at high latitudes during winter. Therefore, the flux needs to be constrained to a high-latitude region and be modulated as a function of time of the year. Because of a lack of data describing the seasonal variation of vertical velocities in the lower thermosphere, the

following time dependency was chosen:

$$F = A_p^{2.5} \cdot c \cdot 2.20 \times 10^5 \text{ cm}^{-2} \text{ s}^{-1} \cdot \max(0.1, \cos(\pi/182.625 \cdot (d - 172.625))) , \quad (4)$$

where d is day of year. This sinusoidal variation centered around solstice represents the minimum requirement of a seasonal variation with maximum in winter. The 10% flux in summer was estimated from HALOE measurements at 0.01 hPa, which indicate elevated NO_x levels during high geomagnetic activity even in summer. A restriction with respect to the latitudes where the flux is applied can be chosen via the Fortran95 namelist of the submodel. There have been findings that enhancements occur down to 30–40° latitude (Siskind et al., 1997). However, Funke et al. (2005) showed that in the middle atmosphere the enhancements are confined to the vortex (their Figs. 5, 6, 7). Therefore we have here used a minimum absolute latitude of 55° representing a conservative estimate. Also possible would be a geomagnetic activity dependent latitudinal extent which has been suggested in the past, but because of other uncertainties this is not likely to improve the results significantly.

In principle, Eq. (4) can be used for any time resolution of the A_p index. Although there has not been any evidence presented that A_p correlates with excess NO_x in the upper mesosphere on shorter time scales, it is very likely that LEE NO_x will follow geomagnetic activity also on shorter timescales than yearly. On the other hand, because of the transport timescales involved (assuming 1 km/day, the transport e.g. from 110 km to 80 km would take 30 days), a resolution higher than approximately one month is unlikely to improve the results. Here, the flux F is calculated from monthly mean values of A_p . The estimated flux is distributed in the form of NO over the top two model levels in order to avoid strong gradients and other undesired effects that could result from introducing the flux into only the top layer, which acts as a sponge layer in the model.

It should be noted that measurements of stratospheric NO_x are only available for a limited number of years. The geomagnetic A_p index in comparison has been measured since 1932 and reconstructions are possible even further into the past (Nagovitsyn, 2006). Therefore, the fact that the presented parametrisation only requires the A_p index as an input function, and is not relying on satellite measurements, is of great advantage for model simulations spanning several decades.

A method often used to prescribe boundary conditions for different types of long-lived gases is to nudge the tracer to a known mixing ratio. In principle, using HALOE data this method would have been feasible to implement. However, the described emission of the tracer is preferable in this case, because otherwise other processes that influence NO_x mixing ratios are overwritten.

In order to assess the capability of the model and the parametrisation to reproduce NO_x mixing ratios in the Northern Hemisphere, the parametrisation was applied there also.

Although the scaling function given by Eq. (3) was developed on the basis of NO_x enhancements in the southern polar region, no changes were made to the parametrisation. Only the time dependency (Eq. 4) was shifted by six months:

$$F = A_p^{2.5} \cdot c \cdot 2.20 \times 10^5 \text{ cm}^{-2} \text{ s}^{-1} \cdot \max(0.1, \cos(\pi/182.625 \cdot (d - 355.25))). \quad (5)$$

The validity of this approach is discussed further in the following section.

3 Results and discussion

In general, the submodel SPACENOX and EMAC can be applied in different setups. In this paper, we will only be concerned with simulations where measured A_p indices are prescribed and the GCM is free running, i.e. the meteorology is not relaxed towards the observed meteorology. Only in this configuration it is possible to perform simulations for many decades, as reliable information on global meteorology only became available with the start of the satellite era. However, as mentioned earlier, the dynamical conditions are an important factor in controlling the amount of NO_x that reaches the stratosphere. Since in this model setup the meteorology, and especially the properties of polar air descent, will be different to the actual meteorology, care needs to be taken when interpreting the results.

In order to evaluate the technique and the submodel, a simulation covering the period 1992 to 2003, forced by corresponding sea surface temperatures and sea-ice coverage, is discussed. From 1992 to September 2002 the “average excess NO_x” scaling, after that the “maximum excess NO_x” scaling was applied as described above. First, the model results for the geomagnetically very active Southern Hemisphere winter 2003 are described and compared to satellite based measurements. Aspects that are addressed include the descent of air inside the polar vortex and characteristics of the LEE NO_x. Then, the interannual variability of LEE NO_x is discussed, and effects on ozone and other constituents are mentioned. Finally, the effects of the parametrisation applied in the Northern Hemisphere are evaluated.

3.1 Southern Hemisphere

3.1.1 Vertical transport

Carbon monoxide, which in the middle atmosphere is mainly produced by photodissociation of CO₂, is used here to show that the model reproduces the general features of vertical transport in the Antarctic. Model results are compared to data from the MIPAS instrument on board ENVISAT, initially presented by Funke et al. (2005), hereafter referred to as F05. MIPAS CO, retrieved by the IMK/IAA (Institut für Meteorologie und Klimaforschung/Instituto de Astrofísica de Andalucía) processor, in the polar vortex is shown as a function

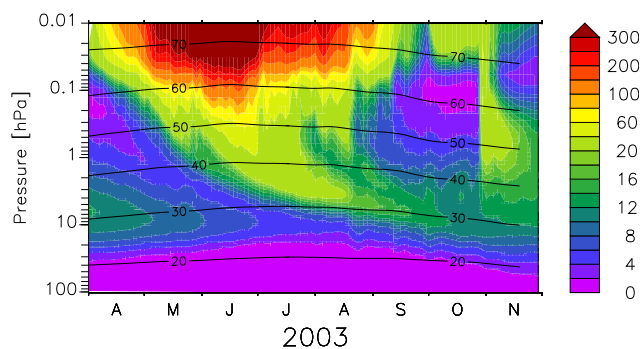


Fig. 3. EMAC NO_x mixing ratios (ppbv) averaged over 60°–90° S for 2003. The contour lines denote the altitude in km.

of time and potential temperature in Fig. 2a (reproduced from F05 Fig. 4c), and corresponding model results are shown in Fig. 2b. In general, the prevailing descent of air maximizing in early winter is reproduced by the model. At potential temperatures above 1500 K agreement is good throughout the winter, however, at lower altitudes and starting in June model CO mixing ratios are too high, indicating that the downward transport is too strong. The implications for the NO_x transport will be discussed later where appropriate. The reasons for this discrepancy are subject to investigations independent of the work presented here.

3.1.2 LEE NO_x in 2003

Figure 3 depicts the simulated mixing ratios of NO_x south of 60°S during 2003. Strong enhancements with mixing ratios of more than 300 ppbv are evident in the mesosphere. They are related to the NO_x produced by the SPACENOX submodel due to the large A_p index during most of the southern winter 2003 (see Fig. 1). Also clearly distinguishable is a sudden enhancement at the end of October. This is related to the solar proton event and is discussed in the companion paper (Baumgaertner et al., 2009). The latitudinal extent of the NO_x enhancements in the Southern Hemisphere winter 2003 is shown in the lower two panels of Fig. 4. In June mixing ratios of more than 200 ppbv extend from the South Pole to 60° S. In the upper stratosphere in August, NO_x enhancements of up to 20 ppbv still reach 60° S. This indicates that NO_x is confined by the polar vortex as expected and will be discussed in more detail below.

Southern polar stratospheric enhancements of NO_x due to downward transport from the upper atmosphere have been presented by F05 using MIPAS measurements for the winter 2003, reproduced here as Fig. 5a. Since these measurements did not form a basis for the parametrisation in any form, the comparison is independent. In order to ease a comparison with F05, potential temperature was chosen as vertical coordinate. This also allowed a consistent transformation to equivalent latitude (Nash et al., 1996). Transformed onto an equivalent latitude, potential vorticity increases (decreases)

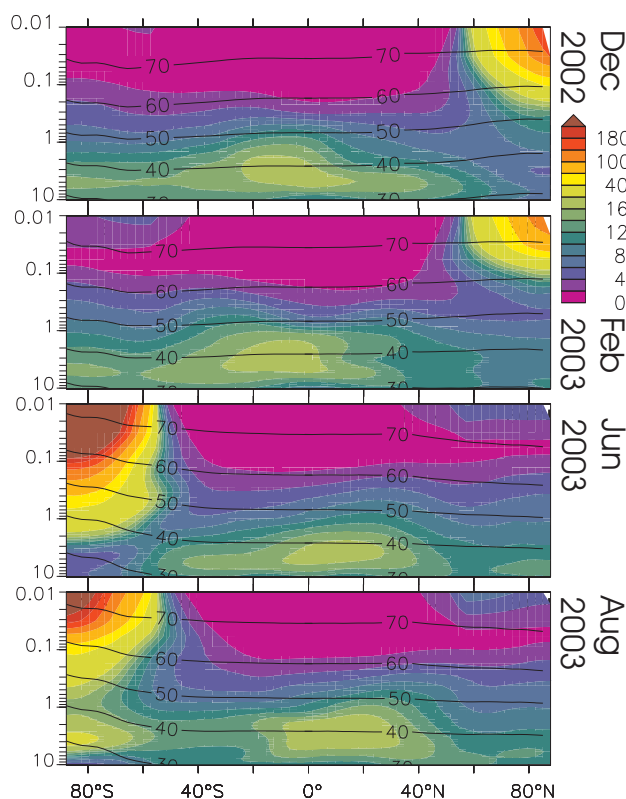


Fig. 4. EMAC NO_x mixing ratios (ppbv) as a function of latitude and pressure level for December 2002, and February, June, and August 2003. The contour lines denote the corresponding altitude in km.

monotonically towards the north (south) pole. This allows a simple determination of the position of a grid box with respect to the edge of the polar vortex. Averaging over regions of high equivalent latitude means only small regions of air outside of the vortex are included. In addition, the vortex edge was calculated from the potential vorticity gradient according to Nash et al. (1996). With this it was possible during every model output timestep to determine the average mixing ratios inside the polar vortex.

NO_x mixing ratios inside the polar vortex are shown in Fig. 5b. Geopotential height was converted to an approximate geometric altitude and is shown as white contours. Downward transport of a NO_x enhancement exceeding 45 ppbv in June/July is clearly discernable and is generally in good agreement with the MIPAS observations with respect to magnitude, timing, and altitude of the enhancements. A NO_x enhancement centered around 2500 K in August is only found in the model results and does not appear in the MIPAS data. Examining the CO abundances inside the vortex, Fig. 2a and b, reveals that in the model a strong descent of mesospheric air occurred during this time, leading to the NO_x enhancements. The MIPAS CO measurements do not show this feature, explaining the difference between model and ob-

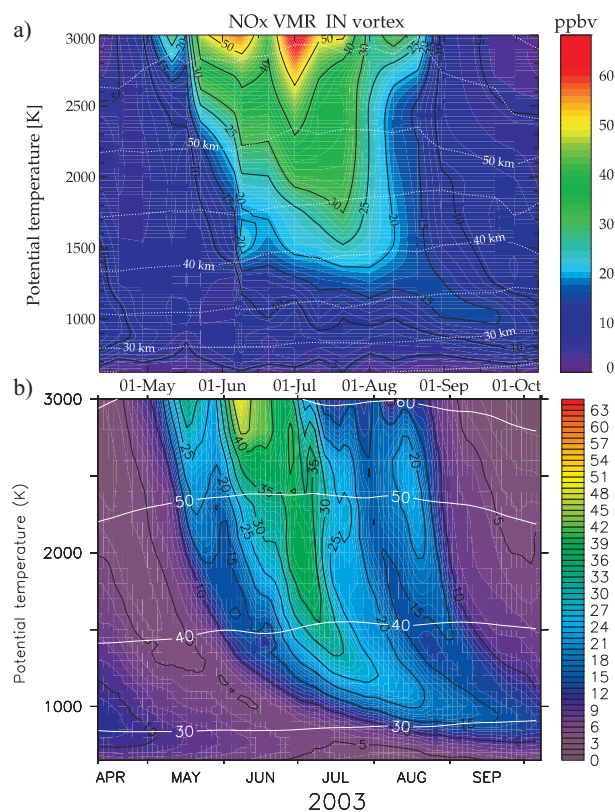


Fig. 5. (a) NO_x mixing ratios inside the southern polar vortex measured by MIPAS (IMK/IAA data). Reproduced from Funke et al. (2005) with kind permission from AGU and B. Funke. (b) EMAC NO_x mixing ratios (ppbv) inside the southern polar vortex during the Southern Hemisphere winter 2003. The vortex edge was defined using the Nash criterion. White contours denote geometric altitudes in km.

served NO_x at this time. As mentioned earlier, the CO measurements and model results also differ below 1500 K from June onwards, with the model showing stronger descent than observed. This difference also explains the higher NO_x mixing ratios in late winter below 1500 K.

3.1.3 LEE NO_x interannual variability

To assess the interannual variability of LEE NO_x, the model results from a simulation covering 1992 to 2003 are compared to the results from R07. Different to the comparison with MIPAS, these data are not independent since the parametrisation was build upon this data. The data for October 2002 to November 2003 are the same as discussed above, however, for 1992 to September 2002 the “average excess NO_x” scaling (see Sect. 2.2) was applied. Therefore, only half of the amount of NO_x was emitted into the model top. Figure 7 of R07, reproduced here as Fig. 6, shows excess NO_x densities at 45 km derived from HALOE data for 1992 to 2005 in 2-week time periods. Since HALOE derived densities in R07 ideally represent estimates for the

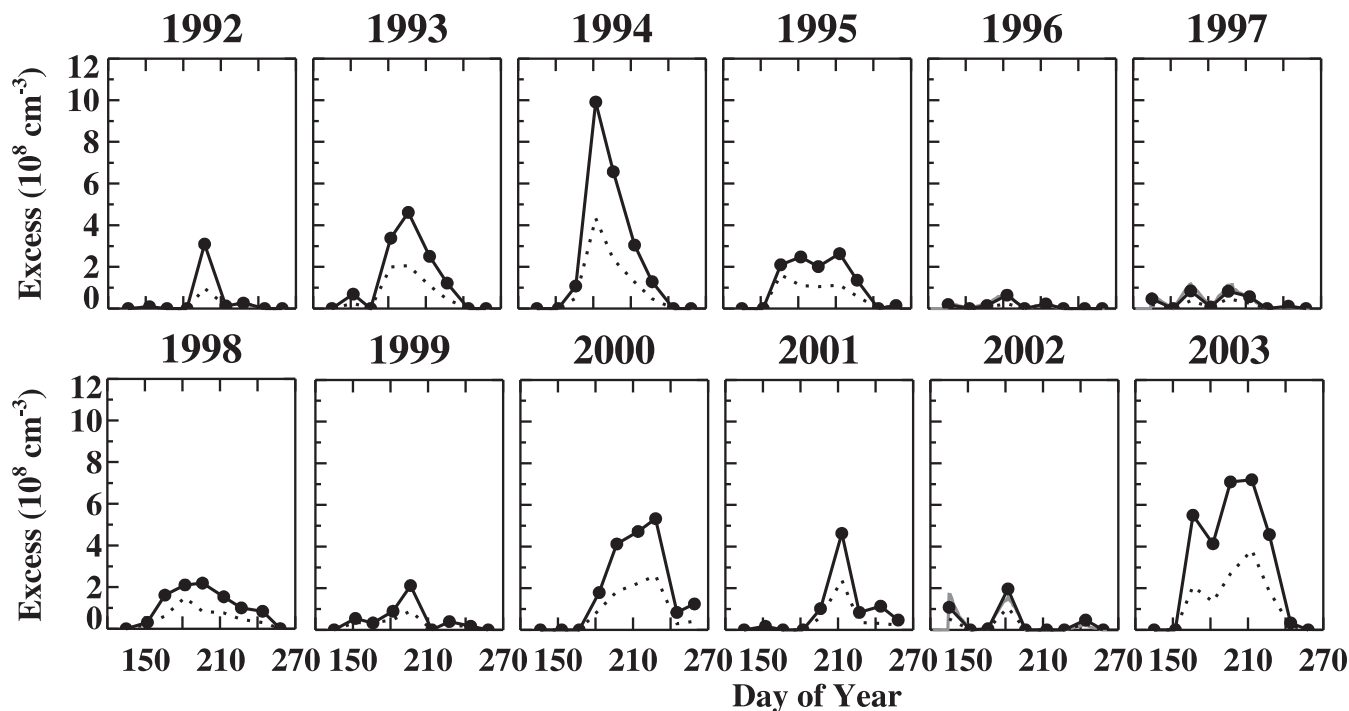


Fig. 6. Maximum (solid) and average (dotted) excess NO_x densities derived from HALOE. Reproduced from Randall et al. (2007) with kind permission from AGU and C. Randall.

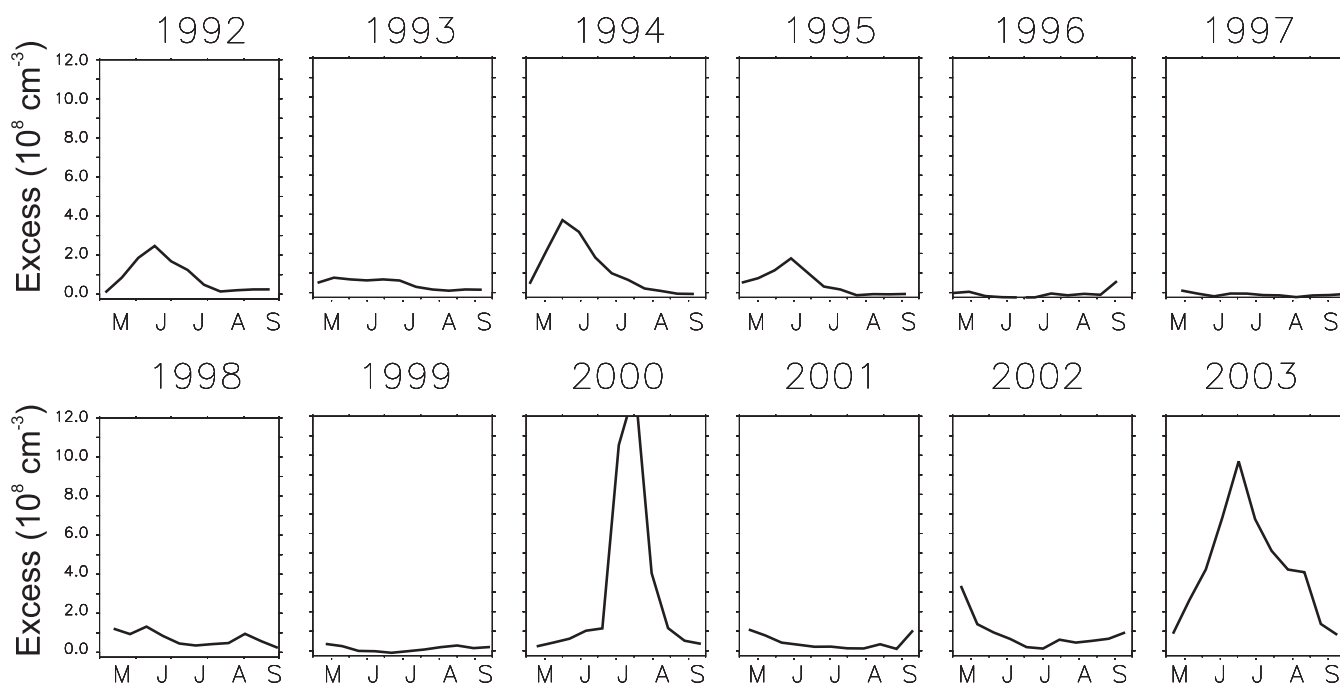


Fig. 7. EMAC excess NO_x densities inside the Southern Hemisphere polar vortex at 45 km. Note that for 1992–2002 the “average excess NO_x” scaling was applied, in 2003 the “maximum excess NO_x” scaling. The vortex edge was defined using the Nash criterion.

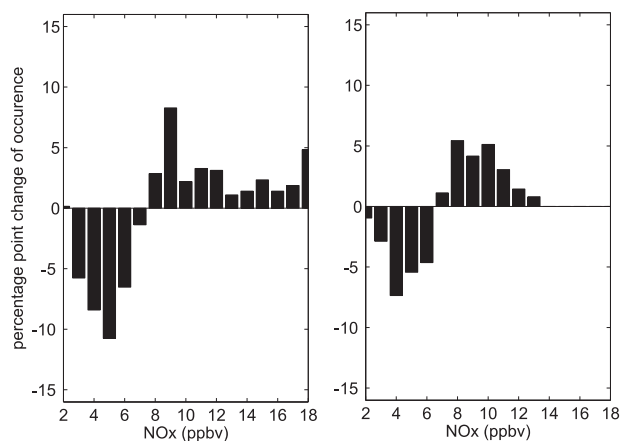


Fig. 8. Difference between the normalised histograms of NO_x mixing ratios at 1 hPa (approx. 45 km) for latitudes south of 40° S during high and low geomagnetic activity (high minus low). Left: HALOE, right: EMAC.

entire vortex region, we have at first not sampled the model output at HALOE measurement locations. Instead NO_x densities were averaged over the area of the polar vortex and averaged in 2-week time periods in accordance with R07. In order to approximate excess densities, $0.75 \times 10^8 \text{ cm}^{-3}$ was subtracted from the absolute densities, which yielded almost no excess NO_x in the years where none is expected due to very low geomagnetic activity. The resulting EMAC excess densities are depicted in Fig. 7. A large interannual variability is evident. Almost no excess NO_x is seen in the years 1993, 1997, and 1999, while large amounts are found in 1994, 2000, and 2003. This is in agreement with the May–July A_p -index (Fig. 1), as expected. There is also a qualitative agreement with excess densities shown in Fig. 6. In a number of years, quantitative agreement is also good. In 2003 maximum excess densities of up to $7 \times 10^8 \text{ cm}^{-3}$ were derived in R07, where the model shows between 6 and approximately $9 \times 10^8 \text{ cm}^{-3}$. Therefore, in 2003 there is good agreement with the maximum excess densities from R07. In the other years, when the “average excess NO_x” scaling was applied, the model agrees better with the average excess densities from R07. However, R07 considered the results based on the maximum excess densities more reasonable. In the light of the good agreement between MIPAS NO_x and the model simulation for 2003 with the “maximum excess NO_x” scaling, this conclusion by R07 is further corroborated.

Concerning a comparison of the temporal behavior of the model excess densities with the results shown in Fig. 6, systematic discrepancies are found. As evident for example in the year 1995, elevated levels of NO_x density in R07 are found until early August, whereas model densities are usually only elevated until early July. There are several possibilities to explain these differences. First, in the model we prescribed a temporal behavior using a cosine function of time

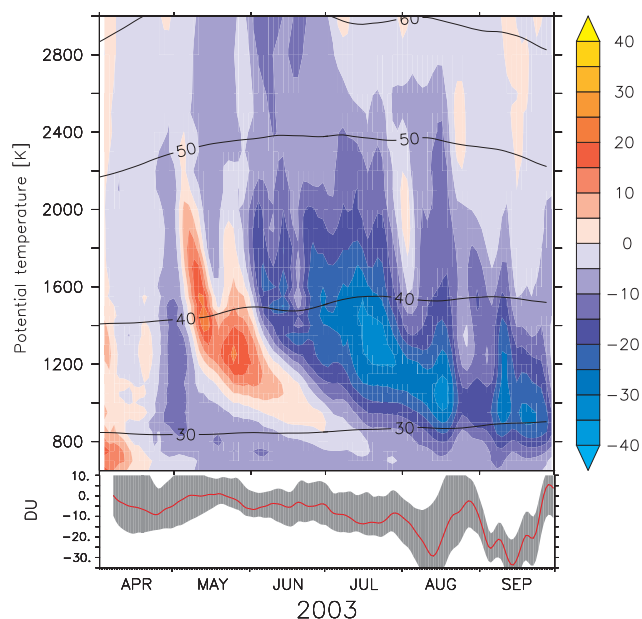


Fig. 9. Top: Ozone change (percent) inside the polar vortex with respect to a simulation with the SPACENOX submodel switched off for the year 2003. The vortex edge was defined using the Nash criterion. The contours denote the approximate altitude in km. Bottom: Total column ozone change. The shaded area denotes the values between the maximum and minimum difference with respect to latitude.

of the year, centered on solstice as described above. This means that statistically NO_x production is largest in June. However, due to the power-law dependency, this is unlikely to be the cause for the large fall-off after the end of June. For example, in 1995, this is clearly attributable to the change in A_p index: In May (June, July, August) the average A_p index was 18.6 (10.2, 7.7, 9.4). Instead, the time shift could mean that the time for the vertical transport between the source region and the model lid cannot be neglected as is done here. This also means that the source region is likely to be significantly higher than the model lid which is located at 0.01 hPa. Introducing a time lag between the A_p -index and the NO_x injection might therefore improve the results and will be subject of future work. A second possible explanation lies in the HALOE sampling as a function of latitude. Until July HALOE measures only up to approx. 50° S, so it only captures NO_x enhancements near the vortex edge and misses the much larger enhancements towards the pole, as discussed by R07. In late winter, the sampling includes latitudes up to 70° S and thus also captures larger NO_x, but at least in some years (e.g. 1995) the bulk of the NO_x enhancements has already been transported to lower altitudes. The convolution of these two aspects could lead to a distorted apparent temporal behavior, i.e. underestimate early winter enhancements and overestimate late winter enhancements, possibly leading to a relatively monotonous enhancement as seen in Fig. 6 in 1995.

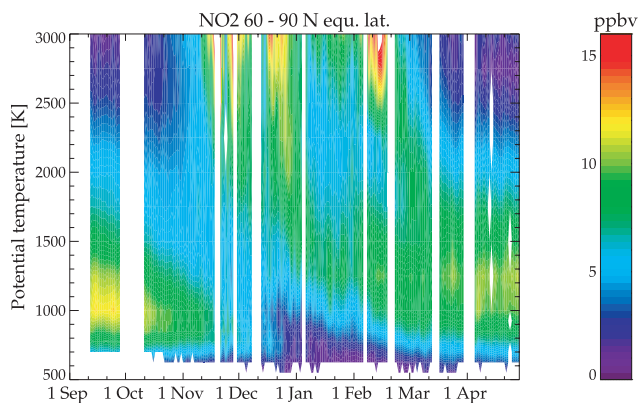


Fig. 10. Nighttime NO₂ mixing ratios measured by MIPAS (ESA data) averaged over 60°–90°N equivalent latitude. Reproduced from Funke et al. (2005) with kind permission from AGU and B. Funke.

A direct point-to-point comparison between model and HALOE (Version 19) NO_x was therefore performed additionally. For this, the model output was sampled at HALOE NO_x measurement locations and at 45 km altitude. Then, normalised histograms were computed for periods of low (winters of 1996, 1997, 1999, 2001, 2002) and high (winters of 1992, 1994, 2000, 2003) geomagnetic activity separately. Finally, the differences between each pair of histograms from the two periods were calculated. The resulting percentage change histograms are shown for HALOE and EMAC in Fig. 8, left and right, respectively. As expected, a shift from lower to higher NO_x values during high geomagnetic activity is evident in both the HALOE data and the model. However, the shift is more pronounced in the observations, again indicating that the applied “average excess NO_x” scaling underestimates NO_x production.

Some of the features evident in Fig. 7 are related to Solar Proton Events. For example, the sudden increase in NO_x density in July 2000 lead to densities up to $11 \times 10^8 \text{ cm}^{-3}$. It is interesting to note that the enhancement in R07 is only half as large. The Solar Proton Event parametrisation is discussed in the companion paper, therefore such features are not discussed further in the present study.

3.1.4 Effects on ozone

Due to the fact that NO_x can engage in catalytic ozone destruction, in the stratosphere significant effects on ozone can be expected during winters with high geomagnetic activity. Therefore EMAC results for the year 2003, where large amounts of NO_x were transported into the southern polar region, are shown here. In Fig. 9 (top panel) the change of ozone mixing ratio inside the polar vortex with respect to the result from a simulation with the submodel SPACENOX switched off is depicted. Depletion of up to 40% follows the downward transport of NO_x as seen in Fig. 5. The bottom

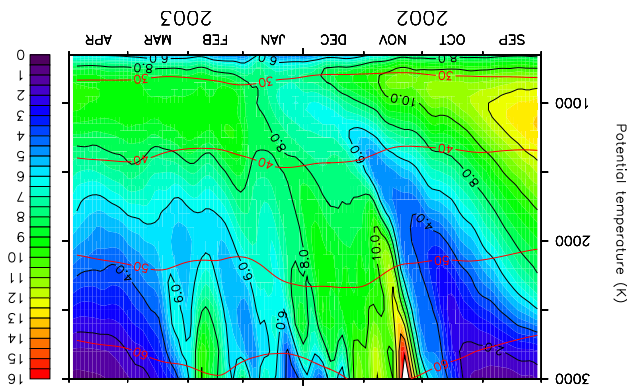


Fig. 11. EMAC NO_x mixing ratios (ppbv) averaged over 60°–90°N equivalent latitude during 2002/2003. The red lines denote geometric altitudes in km.

panel of Fig. 9 shows the total column ozone loss which is also strongly influenced by dynamics. A loss of between 10 and 30 DU appears to be attributable to LEE NO_x. It has to be noted, however, that the overestimation of descent in the polar vortex that was deduced from the CO comparison and also seen in the NO_x comparison potentially implies that the ozone loss is overestimated.

3.1.5 Other effects

Other members of the NO_y family are likely to be affected by the NO_x enhancements. Stiller et al. (2005) provided MIPAS measurements of strong HNO₃ enhancements inside the polar vortex during the Southern Hemisphere winter of 2003. EMAC results for HNO₃ in the same period are smaller by more than one order of magnitude. Since the relevant gas-phase reactions are included in the simulation (see supplement), this indicates that the measured HNO₃ enhancements are likely to result from ion cluster reactions (for more details see Stiller et al., 2005, and the companion paper) that are currently not included in EMAC.

3.2 Northern Hemisphere

For the Northern Hemisphere, where dynamical variability is much larger than in the Southern Hemisphere, additional aspects need to be considered. The larger dynamical variability has a stronger influence on the amount of LEE NO_x deposited in the stratosphere (see e.g. Randall et al., 2005). Variability in the lower thermosphere is not captured in the model simulations and is thus potentially a significant error source. Concerning the upper stratosphere and mesosphere, NO_x transport is exposed to the variability in the model. Therefore, since the model is free running and not reproducing observed dynamical interannual variations, the agreement between model and observed NO_x is worse than by just comparing A_p and measured excess NO_x. On the other hand, if the model reproduces the observed dynamical

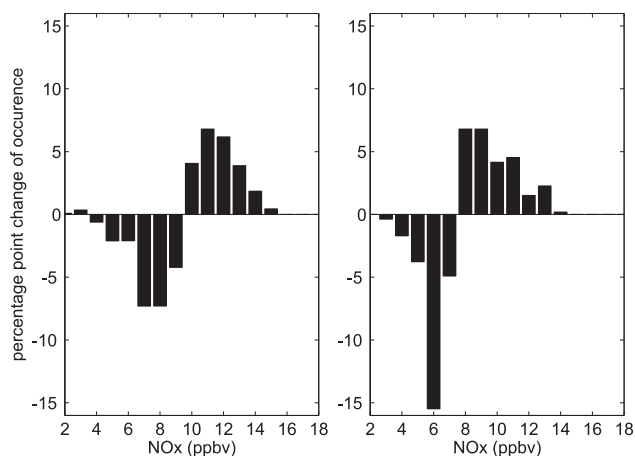


Fig. 12. Same as Fig. 8 but for latitudes north of 40° N. Left: HALOE, right: EMAC.

variability (e.g. by relaxing model meteorology to observed meteorology), the agreement between model and observed NO_x will be better than by just comparing A_p and measured excess NO_x. In the case of the presented model simulations, the model is forced with observed sea surface temperatures, an observed Quasi-Biennial Oscillation (QBO), and observed solar UV radiation. It has been shown by (e.g. Labitzke, 2005) that solar and QBO forcing determine a significant fraction of interannual variability of the vortex, especially the number of mid-winter warmings. This implies that the interannual variability of the Northern Hemisphere vortex in the presented model simulations should show similar features as the observed variability. However, this is still under investigation and beyond the scope of this paper.

The latitudinal extent of LEE NO_x is shown in Fig. 4 for December and February during the Northern Hemisphere winter 2002/03. Mixing ratios up to 100 ppbv are evident from the north pole to 70° N, small enhancements are found up to 40° N. Enhancements in December reach down to 2 hPa.

In order to assess the model's capability to reproduce Northern Hemisphere NO_x mixing ratios, potentially affected by LEE NO_x, we carried out comparisons with satellite data similar to the approach employed for the Southern Hemisphere. F05 also presented measurements from the Northern Hemisphere winter 2002/2003. NO₂ nighttime abundances as a function of equivalent latitude and potential temperature are depicted in their Fig. 12 (top) and are reproduced here as Fig. 10. NO₂ enhancements last from November to February, interrupted by stratospheric warmings. They clearly result from downward transport and reach peak mixing ratios of 16 ppbv. EMAC NO_x mixing ratios for the same period are shown in Fig. 11. Note that the nighttime MIPAS NO₂ only represent a lower limit for NO_x.

Both the model and observations show a strong descent of NO_x starting at 3000 K in November, with mixing ratios of more than 16 ppbv. The excess NO_x is transported down to altitudes of 1500 K (40 km) during the following two months. A second strong enhancement observed by MIPAS in December is not captured by the model. In February, both model and observations again show enhancements above 2500 K, exceeding 16 ppbv in the observations and reaching 10 ppbv in the model. Because of the fact that the main features of the observed NO₂ enhancements are reproduced, we conclude that the parametrisation also works well under moderate dynamical conditions in the Northern Hemisphere, similar to those found in the 2002/2003 winter. Note that the lower altitude enhancements found from January onwards have been shown to be related to midlatitude air that was transported to higher latitudes (see F05), resulting in NO₂ mixing ratios of up to 10 ppbv that last at least until April 2003.

A variety of dynamical conditions can be captured by comparing model NO_x with HALOE observations. Similar to above, normalised NO_x histograms for periods of high (winters of 1991/1992, 1992/1993, 1993/1994, 1994/1995) and low (winters of 1995/1996, 1996/1997, 1997/1998) geomagnetic activity are subtracted and shown in Fig. 12. In general both the HALOE and EMAC data show the shift from low to high NO_x values during geomagnetically active winters, confirming the validity of the parametrisation for a wider range of dynamical conditions.

4 Conclusions

A parametrisation of the production of NO_x in the thermosphere through LEE has been developed with the aim to be able to describe NO_x mixing ratios in the stratospheric polar vortex. The approach is based solely on monthly mean values of the A_p index, which has been shown to be a good proxy for Southern Hemisphere interannual variations of vortex NO_x mixing ratios. A scaling function was developed based on published interannual variations of LEE NO_x derived from HALOE measurements. The technique allows to quantitatively capture measured NO_x enhancements in the stratosphere that are due to LEE precipitation in the thermosphere. The implementation in EMAC was evaluated against independent NO_x measurements by MIPAS for the geomagnetically very active Southern Hemisphere winter 2003 as well as the moderately active Northern Hemisphere winter 2002/03. Excellent agreement was found for both periods. For the Southern Hemisphere winter 2003 a significant impact on ozone was shown. The presented parametrisation of LEE NO_x is therefore a valuable addition to the EMAC AC-GCM and will be useful for simulations of the recent climate. Because the A_p index is available since 1932, it is possible to quantify interannual variability on timescales even longer than satellite measurements of NO_x enhancements due to

LEE. Combined with model implementations of other solar activity dependent processes, namely photolysis, radiative heating, and SPEs, it will be possible to study the holistic impact of solar activity variations on the Earth's atmosphere. Results from an EMAC simulation encompassing these processes and covering the period 1960 until 2003 are in preparation for publication. Due to the success of the technique seen in the presented evaluation and its proven significance on polar ozone chemistry, it is recommended to include such a parametrisation into middle atmosphere AC-GCMs.

Acknowledgements. This research was funded by the ProSECCO project within the DFG SPP 1176 CAWSES. We explicitly acknowledge the work by Randall et al. (2007) which laid the basis for the present study. We thank AGU as well as C. Randall and B. Funke for their kind permission to reproduce figures from their publications. We thank B. Funke for helpful comments on the manuscript. The Ferret program (<http://www.ferret.noaa.gov>) from NOAA's Pacific Marine Environmental Laboratory was used for creating some of the graphics in this paper. Thanks go to all MESSy developers and users for their support.

The service charges for this open access publication have been covered by the Max Planck Society.

Edited by: V. Fomichev

References

- Baumgaertner, A. J. G., Jöckel, P., Riede, H., Brühl, C., Stiller, G., and Funke, B.: Energetic Particle Precipitation in ECHAM5/MESSy1, Part 2: Solar Proton Events, in preparation, Atmos. Chem. Phys. Discuss., 2009.
- Brasseur, G. P. and Solomon, S.: *Aeronomy of the Middle Atmosphere*, D. Reidel Publishing Company, 2nd revised edn., 1986.
- Brühl, C., Steil, B., Stiller, G., Funke, B., and Jöckel, P.: Nitrogen compounds and ozone in the stratosphere: comparison of MIPAS satellite data with the chemistry climate model ECHAM5/MESSy1, Atmos. Chem. Phys., 7, 5585–5598, 2007, <http://www.atmos-chem-phys.net/7/5585/2007/>.
- Callis, L. B. and Lambeth, J. D.: NO_y formed by precipitating electron events in 1991 and 1992: Descent into the stratosphere as observed by ISAMS, Geophys. Res. Lett., 25, 1875–1878, doi:10.1029/98GL01219, 1998.
- Callis, L. B., Natarajan, M., Lambeth, J. D., and Baker, D. N.: Solar - atmospheric coupling by electrons (SOLACE). 2. Calculated stratospheric effects of precipitating electrons, 1979–1988, J. Geophys. Res., 103, 28421–28438, doi:10.1029/98JD02407, 1998.
- Callis, L. B., Natarajan, M., and Lambeth, J. D.: Solar-atmospheric coupling by electrons (SOLACE): 3. Comparisons of simulations and observations, 1979–1997, issues and implications, J. Geophys. Res., 106, 7523–7540, doi:10.1029/2000JD900615, 2001.
- Callis, L. B., Natarajan, M., and Lambeth, J. D.: Observed and calculated mesospheric NO, 1992–1997, Geophys. Res. Lett., 29, 020000–1, doi:10.1029/2001GL013995, 2002.
- Funke, B., López-Puertas, M., Gil-López, S., von Clarmann, T., Stiller, G. P., Fischer, H., and Kellmann, S.: Downward transport of upper atmospheric NO_x into the polar stratosphere and lower mesosphere during the Antarctic 2003 and Arctic 2002/2003 winters, J. Geophys. Res., 110, D24308, doi:10.1029/2005JD006463, 2005.
- Hood, L. L. and Soukharev, B. E.: Solar induced variations of odd nitrogen: Multiple regression analysis of UARS HALOE data, Geophys. Res. Lett., 33, L22805, doi:10.1029/2006GL028122, doi:10.1029/2006GL028122, 2006.
- Jöckel, P., Tost, H., Pozzer, A., Brühl, C., Buchholz, J., Ganzeveld, L., Hoor, P., Kerkweg, A., Lawrence, M. G., Sander, R., Steil, B., Stiller, G., Tanarhte, M., Taraborrelli, D., van Aardenne, J., and Lelieveld, J.: The atmospheric chemistry general circulation model ECHAM5/MESSy1: consistent simulation of ozone from the surface to the mesosphere, Atmos. Chem. Phys., 6, 5067–5104, 2006, <http://www.atmos-chem-phys.net/6/5067/2006/>.
- Labitzke, K.: On the solar cycle-QBO relationship: a summary, J. Atmos. Sol.-Terr. Phys., 67, 45–54, 2005.
- Langematz, U., Grenfell, J. L., Matthes, K., Mieth, P., Kunze, M., Steil, B., and Brühl, C.: Chemical effects in 11-year solar cycle simulations with the Freie Universität Berlin Climate Middle Atmosphere Model with online chemistry (FUB-CMAM-CHEM), Geophys. Res. Lett., 32, L13803, doi:10.1029/2005GL022686, 2005.
- Lelieveld, J., Brühl, C., Jöckel, P., Steil, B., Crutzen, P. J., Fischer, H., Giorgetta, M. A., Hoor, P., Lawrence, M. G., Sausen, R., and Tost, H.: Stratospheric dryness: model simulations and satellite observations, Atmos. Chem. Phys., 7, 1313–1332, 2007, <http://www.atmos-chem-phys.net/7/1313/2007/>.
- Mayaud, P. N.: Derivation, Meaning, and Use of Geomagnetic Indices, Geophysical Monograph 22, Am. Geophys. Union, Washington DC, 1980.
- Nagovitsyn, Y. A.: Solar and geomagnetic activity on a long time scale: Reconstructions and possibilities for predictions, Astron. Lett., 32, 344–352, doi:10.1134/S1063773706050082, 2006.
- Nash, E. R., Newman, P. A., Rosenfield, J. E., and Schoeberl, M. R.: An objective determination of the polar vortex using Ertel's potential vorticity, J. Geophys. Res., 101, 9471–9478, 1996.
- Nissen, K. M., Matthes, K., Langematz, U., and Mayer, B.: Towards a better representation of the solar cycle in general circulation models, Atmos. Chem. Phys., 7, 5391–5400, 2007, <http://www.atmos-chem-phys.net/7/5391/2007/>.
- Randall, C. E., Rusch, D. W., Bevilacqua, R. M., Hoppel, K. W., and Lumpe, J. D.: Polar Ozone and Aerosol Measurement (POAM) II stratospheric NO₂, 1993–1996, J. Geophys. Res., 103, 28361–28372, doi:10.1029/98JD02092, 1998.
- Randall, C. E., Harvey, V. L., Manney, G. L., Orsolini, Y., Codrescu, M., Sioris, C., Brohede, S., Haley, C. S., Gordley, L. L., Zawodny, J. M., and Russell, J. M.: Stratospheric effects of energetic particle precipitation in 2003–2004, Geophys. Res. Lett., 32, L05802, doi:10.1029/2004GL022003, 2005.
- Randall, C. E., Harvey, V. L., Singleton, C. S., Bernath, P. F., Boone, C. D., and Kozyra, J. U.: Enhanced NO_x in 2006 linked to strong upper stratospheric Arctic vortex, Geophys. Res. Lett., 33, L18811, doi:10.1029/2006GL027160, 2006.
- Randall, C. E., Harvey, V. L., Singleton, C. S., Bailey, S. M., Bernath, P. F., Codrescu, M., Nakajima, H., and Russell, J. M.: Energetic particle precipitation effects on the Southern Hemisphere stratosphere in 1992–2005, J. Geophys. Res., 112, D08308, doi:10.1029/2006JD007696, 2007.

- Rinsland, C. P., Salawitch, R. J., Gunson, M. R., Solomon, S., Zander, R., Mahieu, E., Goldman, A., Newchurch, M. J., Irion, F. W., and Chang, A. Y.: Polar stratospheric descent of NO_y and CO and Arctic denitrification during winter 1992–1993, *J. Geophys. Res.*, 104, 1847–1861, doi:10.1029/1998JD100034, 1999.
- Roeckner, E., Brokopf, R., Esch, M., Giorgetta, M., Hagemann, S., Kornbluh, L., Manzini, E., Schlese, U., and Schulzweida, U.: Sensitivity of Simulated Climate to Horizontal and Vertical Resolution in the ECHAM5 Atmosphere Model, *J. Climate*, 19, 3771, doi:10.1175/JCLI3824.1, 2006.
- Roazanov, E., Callis, L., Schlesinger, M., Yang, F., Andronova, N., and Zubov, V.: Atmospheric response to NO_y source due to energetic electron precipitation, *Geophys. Res. Lett.*, 32, L14811, doi:10.1029/2005GL023041, 2005.
- Rusch, D. W., Gérard, J.-C., Solomon, S., Crutzen, P. J., and Reid, G. C.: The effect of particle precipitation events on the neutral and ion chemistry of the middle atmosphere-I. Odd nitrogen, *Planet. Space Sci.*, 29, 767–774, doi:10.1016/0032-0633(81)90048-9, 1981.
- Russell, III, J. M., Rinsland, C. P., Farmer, C. B., Froidevaux, L., Toon, G. C., and Zander, R.: Measurements of odd nitrogen compounds in the stratosphere by the ATMOS experiment on Space-lab 3, *J. Geophys. Res.*, 93, 1718–1736, 1988.
- Sander, R., Kerkweg, A., Jöckel, P., and Lelieveld, J.: Technical note: The new comprehensive atmospheric chemistry module MECCA, *Atmos. Chem. Phys.*, 5, 445–450, 2005, <http://www.atmos-chem-phys.net/5/445/2005/>.
- Seppälä, A., Clilverd, M. A., and Rodger, C. J.: NO_x enhancements in the middle atmosphere during 2003–2004 polar winter: Relative significance of solar proton events and the aurora as a source, *J. Geophys. Res.*, 112, L23303, doi:10.1029/2006JD008326, 2007.
- Siskind, D. E., Bacmeister, J. T., Summers, M. E., and Russell, III, J. M.: Two-dimensional model calculations of nitric oxide transport in the middle atmosphere and comparison with Halogen Occultation Experiment data, *J. Geophys. Res.*, 102, 3527–3546, doi:10.1029/96JD02970, 1997.
- Siskind, E., Nedoluha, G. E., Randall, C. E., Fromm, M., and Russell, III, M.: An assessment of Southern Hemisphere stratospheric NO_x enhancements due to transport from the upper atmosphere, *Geophys. Res. Lett.*, 27, 329–332, doi:10.1029/1999GL010940, 2000.
- Stiller, G. P., Mengistu Tsidu, G., von Clarmann, T., Glatthor, N., Höpfner, M., Kellmann, S., Linden, A., Ruhnke, R., Fischer, H., López-Puertas, M., Funke, B., and Gil-López, S.: An enhanced HNO₃ second maximum in the Antarctic midwinter upper stratosphere 2003, *J. Geophys. Res.*, 110, 20303, doi:10.1029/2005JD006011, 2005.
- Vogel, B., Konopka, P., Groß, J.-U., Müller, R., Funke, B., López-Puertas, M., Reddmann, T., Stiller, G., von Clarmann, T., and Riese, M.: Model simulations of stratospheric ozone loss caused by enhanced mesospheric NO_x during Arctic Winter 2003/2004, *Atmos. Chem. Phys.*, 8, 5279–5293, 2008, <http://www.atmos-chem-phys.net/8/5279/2008/>.